Earth Syst. Sci. Data, 9, 149–162, 2017
www.earth-syst-sci-data.net/9/149/2017/
doi:10.5194/essd-9-149-2017

Open Access Earth System Science Data

Reconstruction of spatially detailed global map of NH_4^+ and NO_3^- application in synthetic nitrogen fertilizer

Kazuya Nishina, Akihiko Ito, Naota Hanasaki, and Seiji Hayashi

National Institute for Environmental Studies, Tsukuba, Ibaraki 305-8604, Japan

Correspondence to: Kazuya Nishina (nishina.kazuya@nies.go.jp)

Received: 3 June 2016 – Discussion started: 25 July 2016
Revised: 31 January 2017 – Accepted: 2 February 2017 – Published: 20 February 2017

Abstract. Currently, available historical global N fertilizer map as an input data to global biogeochemical model is still limited and existing maps were not considered NH_4^+ and NO_3^- in the fertilizer application rates. This paper provides a method for constructing a new historical global nitrogen fertilizer application map (0.5° × 0.5° resolution) for the period 1961–2010 based on country-specific information from Food and Agriculture Organization statistics (FAOSTAT) and various global datasets. This new map incorporates the fraction of NH_4^+ (and NO_3^-) in N fertilizer inputs by utilizing fertilizer species information in FAOSTAT, in which species can be categorized as NH_4^+- and/or NO_3^--forming N fertilizers. During data processing, we applied a statistical data imputation method for the missing data (19 % of national N fertilizer consumption) in FAOSTAT. The multiple imputation method enabled us to fill gaps in the time-series data using plausible values using covariates information (year, population, GDP, and crop area). After the imputation, we downscaled the national consumption data to a gridded cropland map. Also, we applied the multiple imputation method to the available chemical fertilizer species consumption, allowing for the estimation of the NH_4^+ / NO_3^- ratio in national fertilizer consumption. In this study, the synthetic N fertilizer inputs in 2000 showed a general consistency with the existing N fertilizer map (Potter et al., 2010) in relation to the ranges of N fertilizer inputs. Globally, the estimated N fertilizer inputs based on the sum of filled data increased from 15 to 110 Tg-N during 1961–2010. On the other hand, the global NO_3^- input started to decline after the late 1980s and the fraction of NO_3^- in global N fertilizer decreased consistently from 35 to 13 % over a 50-year period. NH_4^+-forming fertilizers are dominant in most countries; however, the NH_4^+ / NO_3^- ratio in N fertilizer inputs shows clear differences temporally and geographically. This new map can be utilized as input data to global model studies and bring new insights for the assessment of historical terrestrial N cycling changes. Datasets available at doi:10.1594/PANGAEA.861203.

1 Introduction

Terrestrial nitrogen cycling is significantly governed by human activities (Galloway et al., 2004). The estimated global N loadings to ecosystems likely overload their N capacity (Rockström et al., 2009; De Vries et al., 2013; Steffen et al., 2015). The anthropogenic reactive N (Nr) loadings to terrestrial ecosystems have become twice that of the estimated biogenic N fixation in terrestrial ecosystems in the late 20th century (Gruber and Galloway, 2008). Synthetic nitrogen fertilizers and fossil fuel combustion are, respectively, the first and second largest anthropogenic sources of Nr to terrestrial ecosystems (Galloway et al., 2003, 2008). Excessive Nr in the applies synthetic N fertilizer remains in the environment without crop uptake (Liu et al., 2010; Conant et al., 2013) and contributes to an overabundance of Nr – eutrophication, N saturation – in various ecosystems (Galloway et al., 2003). Also, anthropogenic Nr alters atmosphere–biosphere Nr exchanges via compounds such as N_2O, NH_3, and NO_x (Mosier et al., 1998; Galloway et al., 2004; Davidson, 2009; Tian et al., 2016).

The use of synthetic nitrogen fertilizers grew rapidly after the birth of the Haber–Bosch technique and especially in the latter half of the 20th century (Galloway et al., 2003;

Erisman et al., 2008; Sutton and Bleeker, 2013). The N fertilizer applied to cropland soils – Nr – transfers and is lost to the environment (atmosphere, hydrosphere) with an environment-specific retention time (Galloway et al., 2003). The fertilizer Nr input to terrestrial ecosystems is expected to increase during the 21st century due to increases in the world population and economic growth (Erisman et al., 2008; Davidson, 2012; Bouwman et al., 2013). However, there are still large uncertainties with regard to the historical cumulative Nr impacts on terrestrial ecosystem at the global scale. The N loading capacity of terrestrial ecosystems differs among regions due to differing climates and capacities of ecosystems (Steffen and Smith, 2013; De Vries et al., 2013). Therefore, spatiotemporal information may be important for assessing Nr impacts on terrestrial N cycling. Currently, global synthetic N fertilizer maps are available (Potter et al., 2010; Mueller et al., 2012) only for the year 2000.

The type of synthetic fertilizer is an important factor affecting gaseous Nr release and leaching from croplands because different types of synthetic fertilizers have different chemical characteristics and bioavailability to microbes and crops. For example, when considering the amount of NH_3 volatilization from N-fertilized soils, whether the fertilizer contains ammonium salts (NH_4^+) or whether it is a NH_4^+-forming N fertilizer such as urea is a critical regulation factor in relation to Nr loss (Harrison and Webb, 2001; Bouwman et al., 2002). Also, the type of fertilizer (e.g., nitrate salts, ammonium salts and urea, or anhydrous NH_4^+) determines other N oxide gas emissions from fertilized soil (Bouwman, 1996; Harrison and Webb, 2001; Shcherbak et al., 2014). Early work by Matthews (1994) considered the types of N fertilizer in FAO statistics for the global estimation of NH_4; however, to the authors' knowledge, there are no available historical N fertilizer maps that consider the type of N on a global basis. To assess Nr impacts on terrestrial N cycling in more detail, historical maps of the amounts of NH_4^+ and NO_3^-, as well as N deposition for different N forms, are required (Shindell et al., 2013).

Global national statistics (national survey data) consist of time-series cross-section datasets (i.e., those with years of data for each country). The major issue in the available national statistics for N fertilizer (FAOSTAT, IFA dataset) is that the reported data have many missing values for a significant number of country-years. Excluding those countries with insufficient observations would reduce the number of available countries and lead to a fragmented global historical map. Regular gridded spatiotemporally continuous data of NH_4^+ and NO_3^- are essential for global terrestrial models including biogeochemical models, crop growth models, and many others. To avoid the missing data problem, various data imputation methods have recently been developed. In particular, for time-series cross-section datasets, a statistical imputation method called "Amelia" (King et al., 2001) has succeeded in effectively filling missing values in social studies (e.g. Ross, 2006; Evans et al., 2010; Honaker and King, 2010) and natural sciences (Pyšek et al., 2015). This method would also be suitable for missing values in an N fertilizer consumption dataset.

In this study, to facilitate historical N impact studies at a global scale, we produced a new global N fertilizer input map. This was a spatiotemporal explicit map for 1960–2010 that considered the fraction of NH_4^+ and NO_3^- in the N fertilizer inputs. Using country statistics in FAOSTAT (Food and Agriculture Organization of the United Nations, 2014) for 1960–2010 (subsequently filled using the statistical imputation method), we downscaled the data into $0.5° \times 0.5°$ maps with historical cropland maps (Hurtt et al., 2011). To evaluate such maps, we compared them with the existing global N fertilizer map for the year 2000 and an N deposition map (Shindell et al., 2013).

2 Materials and methods

We used country-based statistics of N fertilizer consumption from the FAOSTAT data (Food and Agriculture Organization of the United Nations, 2014). We summarize the data processing protocol for the total N fertilizer map in Fig. 1. The detailed protocol is as follows.

2.1 Manual cleaning and processing of FAOSTAT data

All available data for each country during the years 1961–2010 were used in this study. Issues in the reported FAOSTAT data (e.g., data referring to imports only or data expressed in formulated products) were evaluated case by case and unreliable data were considered as missing data. For some countries (e.g., the former Soviet Union, the Socialist Federal Republic of Yugoslavia, Eritrea, Ethiopia, and the Czechoslovak Republic), the national statistics were separated due to the change in the framework of these nations from 1960 to 2010. In order to maintain consistency in the national statistics before and after the change in political system, we used the framework in 2000. To avoid discontinuity in the statistics before and after the frame change, we used the trends in the former frameworks and then weighted the N fertilizer consumptions.

2.2 Data imputation for missing data in the national fertilizer consumption statistics

Before the downscaling processes for the global N fertilizer map, we applied statistical data imputation to the FAOSTAT data. This was done because there were many missing values, especially for developing countries. For data imputation, we used the multiple data imputation method for time-series cross-section datasets proposed by King et al. (2001). This was based on a bootstrap-based expectation-maximization algorithm with an assumption of a multivariate normal distribution among covariates. The basic concept of statistical

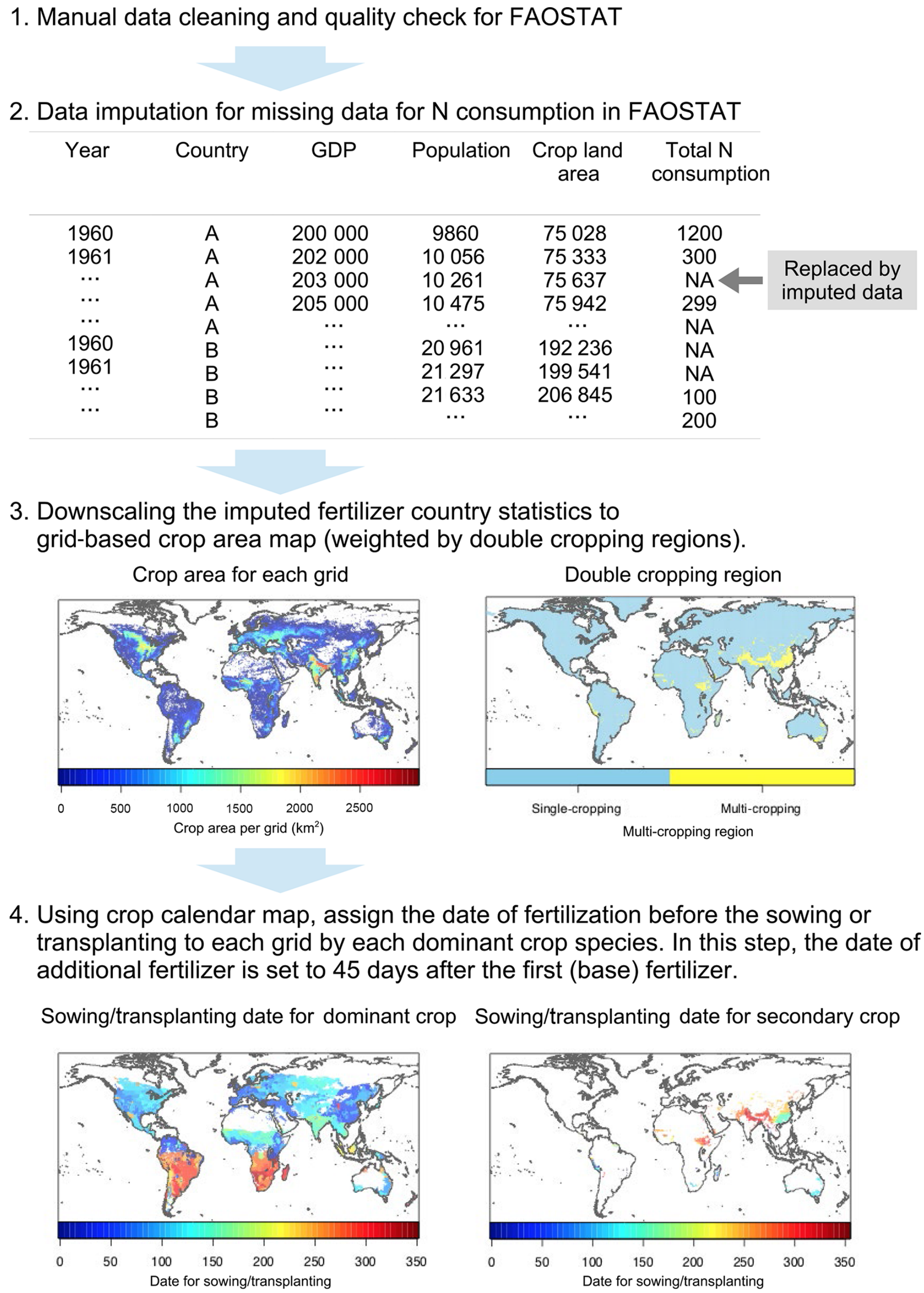

Figure 1. Flow diagrams for downscaling national N fertilizer consumption data to gridded map in this study. Crop area map is LUHa v1.0 (Hurtt et al., 2011). Multi-cropping regions are calculated from Siebert et al. (2010). Dates for sowing and transplanting are obtained from SAGE dataset (Sacks et al., 2010).

data imputation is as follows:

$$D \sim \mathcal{N}_k(\boldsymbol{\mu}, \boldsymbol{\Sigma}), \tag{1}$$

where D is a dataset with n observations and k variables. $\mathcal{N}_k(\boldsymbol{\mu}, \boldsymbol{\Sigma})$ indicates k dimensions of a multivariate normal distribution with a mean vector $\boldsymbol{\mu}$ and $k \times k$ covariance matrix $\boldsymbol{\Sigma}$.

In statistical data imputation, the missing dataset is assumed to be the conditional probability of the observed dataset (D^{obs}), which is equivalent to the conditional probability of the whole dataset D (including the missing dataset D^{miss}) as follows:

$$p(\mathbf{M}|D) = p(\mathbf{M}|D^{\mathrm{obs}}), \tag{2}$$

where $\mathbf{M}$ indicates the $n \times k$ missingness matrix, that is, each element equals 1 if the corresponding element of D is missing and equals 0 if it is observed. This is based on the assumption that data are missing at random. According to this assumption, the estimation of parameters in the multivariate normal distribution for D^{obs} enables the estimation of D^{miss}. In this study, we used the R package "Amelia" for statistical imputation (Honaker et al., 2011). This program has an advanced statistical imputation protocol to handle time-series and cross-sectional features of panel data; this is preferable to nation-based statistics. Amelia incorporates time-series smoothing for the imputed data using various algorithms such as polynomial, spline, and locally weighted scatterplot smoothing functions. In this package, to estimate $\boldsymbol{\mu}$, $\boldsymbol{\Sigma}$ for D^{obs}, a bootstrap-based expectation-maximization algorithm was used by optimizing $L(\boldsymbol{\mu}_{\mathrm{ob}}, \boldsymbol{\Sigma}_{\mathrm{ob}}|D^{\mathrm{obs}})$ as a posterior with flat priors (Honaker and King, 2010). Therefore, the iterative sampling from the posterior of the parameter enables the generation of multiple datasets for the missing data. Across the multiple datasets, the variance in the imputed values by bootstrapping reflects Amelia's uncertainty over the observation's true value.

We applied this algorithm to the national N fertilizer consumption dataset in FAOSTAT. The covariates used were national GDP (from World bank), national population (FAOSTAT), and national cropland area. The historical cropland area in each nation was calculated from the Harmonized Global Land Use map (LUHa) v1.0 (Hurtt et al., 2011). Before application of the data imputation, we converted the N fertilizer consumption to a proportion (0 to 1) by dividing the maximum N fertilizer value during 1960–2010 in each country. This procedure enabled us to constrain the imputed values in the N consumption to less than the existing values. Therefore, we used a logistic transformation for the imputation in Amelia to satisfy the multivariate normal distribution. Furthermore, we used a three-order polynomial function to smooth the missing values over time within a country (Honaker and King, 2010). In this study, we generated 1000 "complete" datasets and then took an ensemble average for the generated dataset as a final complete dataset.

2.3 Downscaling the filled dataset of the national inventory to a spatially explicit map

To downscale the imputed national N fertilizer consumption data to the 0.5° × 0.5° grid-based map, we used the cropland fraction of each grid cell in the LUHa v1.0 map, which provides land-use maps for 1901–2007 (Hurtt et al., 2011). For the period 2008–2010, we repeatedly used the 2007 map in LUHa v1.0. Before the assignment of N fertilizer inputs in each grid, we calculated the time series of N fertilizer rates for each country k. This can be calculated from the balance between national N fertilizer consumption and national cropland area in each year (see examples in Fig. 2). In this study, we considered double cropping regions at both rates and timings of N fertilizer input as follows:

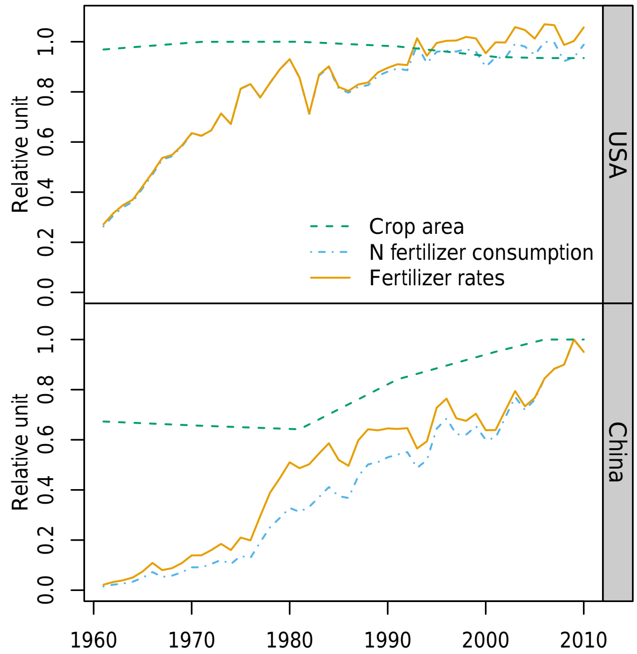

Figure 2. Example of determination of time-series fertilizer application rates in USA and China. For both national crop area and N fertilizer consumption, the values are divided by the maximum for this period. Hence, the unit of fertilizer rates is non-dimension in this figure.

$$\mathrm{Ndose}_{k,t} = \frac{\mathrm{Ncons_{k,t}}}{\sum\limits_{i,j} \mathrm{Carea}_{k,t,i,j} W_{i,j}}, \quad k \in i, j, \tag{3}$$

where $\mathrm{Ndose}_{k,t}$ indicates the N fertilizer input rate (kg-N ha^{-1}) for country k at year t (ranges from 1961 to 2010). $\mathrm{Ncons}_{k,t}$ is the national N fertilizer consumption (kg-N) of country k at year t. Imputed data were used for $\mathrm{Ncons}_{k,t}$ in place of missing data. $\mathrm{Carea}_{k,t,i,j}$ is the cropland area for country k at year t, which was based on the LUHa v1.0 map. $W_{i,j}$ indicates the weight matrix at latitudinal i and longitudinal j positions in the corresponding country k. If the position at i, j is a double cropping region, the value is 2; otherwise, the value is 1 for $W_{i,j}$. This is based on the crop calendar for double cropping species in the SAGE dataset (Sacks et al., 2010), which considered winter (spring) barley, winter (spring) oats, winter (spring) wheat, second rice crop, second maize sorghum, and second sorghum in this study (see map in protocol 3 of Fig. 1). The double cropping regions were determined from global crop use intensity (CUI) map developed by Siebert et al. (2010). We defined the double cropping regions in our map as those where the CUI was greater than 1.3. In this region, we doubled the crop area (i.e., the weighting W_{ij} were set to be 2 in the double cropping region) for the entire 1961 to 2010 period.

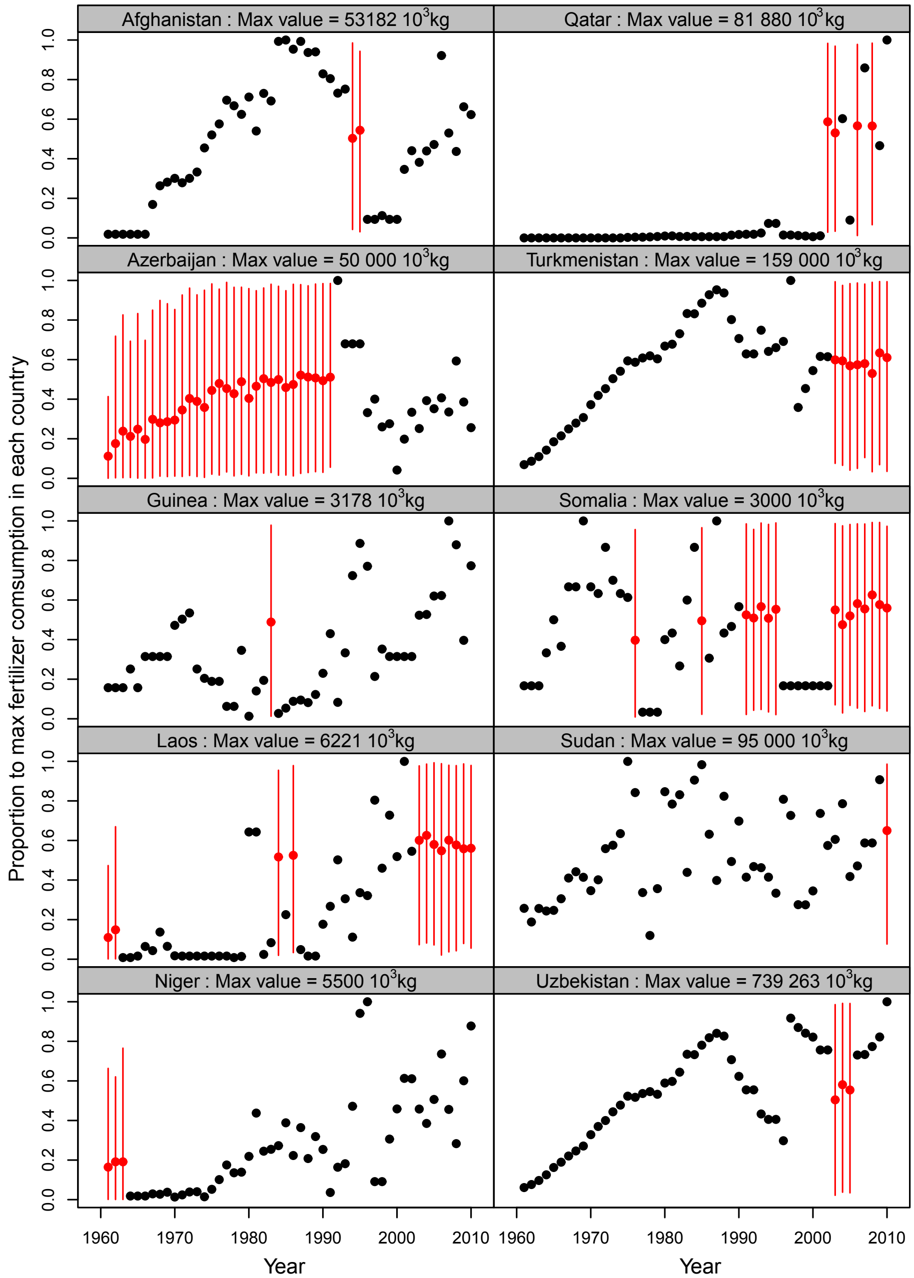

Figure 3. Example of imputation for missing data in national fertilizer consumption data in FAOSTAT. Black points are observed values of the time series and red points are the mean imputed data for missing values. Error bars indicate the 95 % confidence interval obtained using 1000-times bootstrapped data.

2.4 Assignment of fertilizer input date using crop calendar map

Using M3-Crops Data (Monfreda et al., 2008), we determined the dominant cropping species in each grid cell from a choice of 19 species (barley, cassava, groundnuts, maize, millet, oats, potato, pulses, rapeseed, rice, rye, sorghum, soybean, sunflower, sweet potato, wheat, and yam). Next, we used the Crop Calendar in the SAGE dataset (Sacks et al., 2010) and determined the schedule of N fertilizer input in each grid cell using the dominant crop species. The selected species is the most common species between the two databases. For the double cropping regions, we considered seven cropping species, as described in the previous section (2.3). The maps for the sowing/transplanting date are shown in Fig. 1 in protocol 4. To merge the crop calendar maps and fertilizer input map, we applied linear interpolation to the main crop calendar map (except for cases of double crop-

Table 1. Composition of N types in each fertilizer species that appeared in FAOSTAT.

Fertilizer type	$NH_4^+ : NO_3^-$	Global cons* [Tg]
Ammonium nitrate	50 : 50	5.46
Ammonium phosphate	100 : 0	4.64
Ammonium sulfate	100 : 0	2.67
Ammonium sulfate nitrate	75 : 25	0.02
Calcium cyanamide	100 : 0	0.02
Calcium ammonium nitrate	50 : 50	3.25
Calcium nitrate	0 : 100	0.10
Sodium nitrate	0 : 100	0.02
Urea	100 : 0	40.20
Other N	100 : 0	15.67

Other N (e.g., N, P, K mixture; nitrogenous fertilizer). The ratio of Other N is an assumed value. * Global consumption is the values in year 2000 in FAOSTAT without the application of statistical imputation.

ping regions) against each latitudinal band. This procedure enabled us to avoid a mismatch of cropland area between the maps. For the assignment of fertilizer inputs, base fertilizer application was set at 7 days before sowing/transplanting and second fertilizer application was set at 45 days after the base fertilizer application. We assumed the ratio between the base and second fertilizer applications was 7 : 3. In the grid cell for the double cropping regions, we assigned "$\mathrm{Ndose}_{k,t}$" twice for each cropping duration. The dates of N fertilizer inputs were fixed during 1960–2010.

2.5 Allocation of total N fertilizer dose to NH_4^+ and NO_3^- inputs

The statistics for various types of synthetic fertilizer consumption are available in FAOSTAT. These can be sorted by the content (forming) of NH_4^+ and NO_3^-. We converted total N fertilizer input to NH_4^+ and NO_3^- inputs based on the fertilizer species composition. Table 1 summarizes the N-based ratio of NH_4^+ and NO_3^- contents (or forming in soils) in each fertilizer species. Before the imputation, we manually applied data cleaning – i.e., unreliable data (e.g., order of magnitude inflation for just 1 year) were discarded and treated as missing data. If information about a certain fertilizer type in a certain country was unavailable, we replaced zero instead of missing value during such periods.

In the same manner as for the national fertilizer consumption, we applied Amelia to the missing data for the multiple fertilizer species consumption. However, for the fertilizer species, we did not apply the data conversion to the proportion. Instead, we used square root transformation in the Amelia program to maintain positive values in the imputed values. For the covariates, we used the imputed national N fertilizer consumption (obtained as above) and 10 types of fertilizer species as in Table 1. Also, we used a third-order polynomial function to smooth the missing values over time within a country using Amelia (Honaker and King, 2010). We generated 1000 "complete" datasets and then took an ensemble average and standard deviation of the generated dataset as the imputation dataset.

After imputation, we calculated the ratio of NH_4^+ to NO_3^- from the sum of each fertilizer species according to contents of NH_4^+ and NO_3^- (Table 1) as follows:

$$\mathrm{NH4frac}_{k,t} = \frac{\sum_m a_m \mathrm{Fert}_{k,t,m}}{\sum_m \mathrm{Fert}_{k,t,m}}, \quad k \in i, j, \tag{4}$$

where m indicates the type of fertilizer considered in this study (Table 1), NH4frac is the NH_4^+ fraction for each k country at year t, a_m is the coefficient of NH_4^+ fraction to total N in each m fertilizer species (see in Table 1), and $\mathrm{Fert}_{k,t,m}$ indicates the amount of consumption of each imputed fertilizer species for each country in year t. When information about a country was not available, we used the smoothed regional average, for which the regions were defined as Asia, Australia, Europe, North America, Latin America, North Africa, Sub-Sahara, and Pacific Islands.

Finally, we applied spline smoothing to $\mathrm{NH4frac}_{k,t}$ in the filled time-series dataset in each country k to ensure smoothness over time. This is because even the existing data for each fertilizer species seemed unreliable (e.g., round figures, 1 or 2 significant figures) and $\mathrm{NH4frac}_{k,t}$ was discontinuous change across years in some countries. This procedure obtained smoothness over time for each country and also preserved trends in the consumption of fertilizer species.

3 Results and discussion

The key characteristics of the developed N fertilizer map are twofold: (1) it includes time-series information owing to statistical imputation of missing records in the fertilizer census, and (2) it includes the NH_4^+ / NO_3^- ratio. In the following sections, we introduce and validate the developed N fertilizer map, focusing particularly on these two characteristics.

3.1 Visual checking of imputed data and their trends

Examples of the imputed data are visualized in Fig. 3. The percentage of missing values in the national N consumption data was 16 % of a total of 9811 values. As a result of statistical data imputation, the mean of the imputed data was seemingly reasonable for the major countries (Fig. 3). In the imputation procedure, we used logistic transformation after the scaling N fertilizer consumptions by the observed maximum value of each country for the period 1961–2010. This procedure has the potential to underestimate the total N fertilizer consumption in each country; however, the missing values are likely to occur in the early period (during 1961–2010), whereas statistics for recent years are usually available for

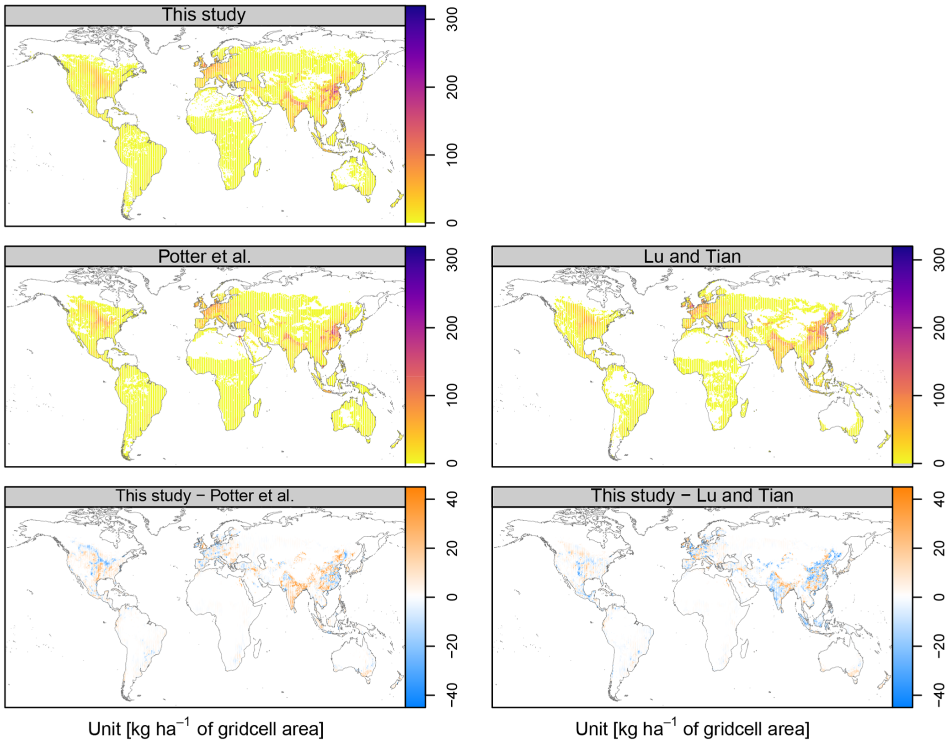

Figure 4. Comparison of total N fertilizer inputs in year 2000. This study's map was obtained by the sum of NH_4^+ and NO_3^- inputs (doi:10.1594/PANGAEA.861203). Left and right middle maps were obtained from Potter et al. (2010) and Lu and Tian (2016), respectively. The lower panels were produced by the subtraction of reference maps from this study's map.

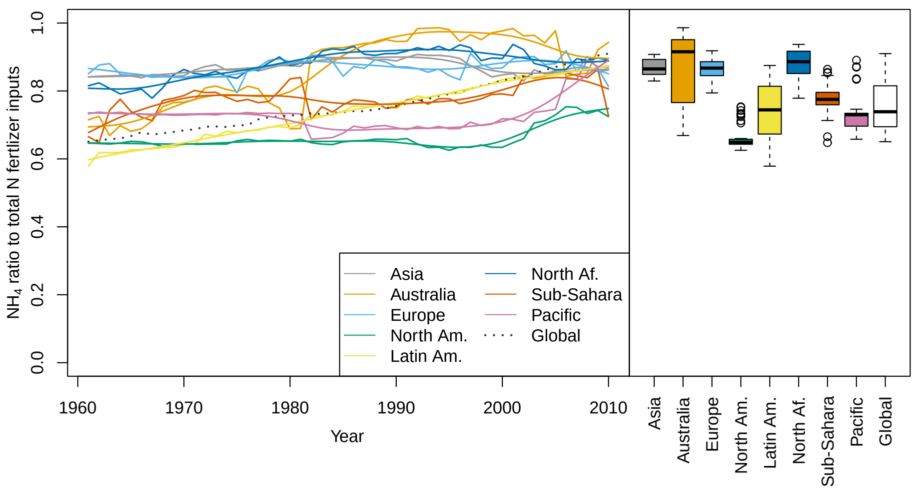

Figure 5. Regional fraction of NH_4^+ in N fertilizer input during 1961–2010. The box plot summarizes the values over the entire period. The upper and lower borders of each box mark the means of the 25th and 75th percentiles, respectively. Open circles represent outliers if the largest (or smallest) value is greater (or less) than 1.5 times the box length from the 75th percentile (or 25th percentile).

almost all countries. In addition, the N fertilizer consumption increases with time. Thus, this procedure can avoid the imputed values being an unreasonable underestimation.

The missing data in FAOSTAT actually did not follow a random pattern; for example, all data for Azerbaijan before 1990 were missing. However, even for such countries, the mean imputed data given by Amelia seemed to makes sense. For example, the trend in the mean imputation data in Azerbaijan was similar to that in Turkmenistan (Fig. 3). Amelia allows for smooth time trends, shifts across cross-sectional units, and correlations over time and space in the imputation (Honaker and King, 2010). Furthermore, Amelia can take ad-

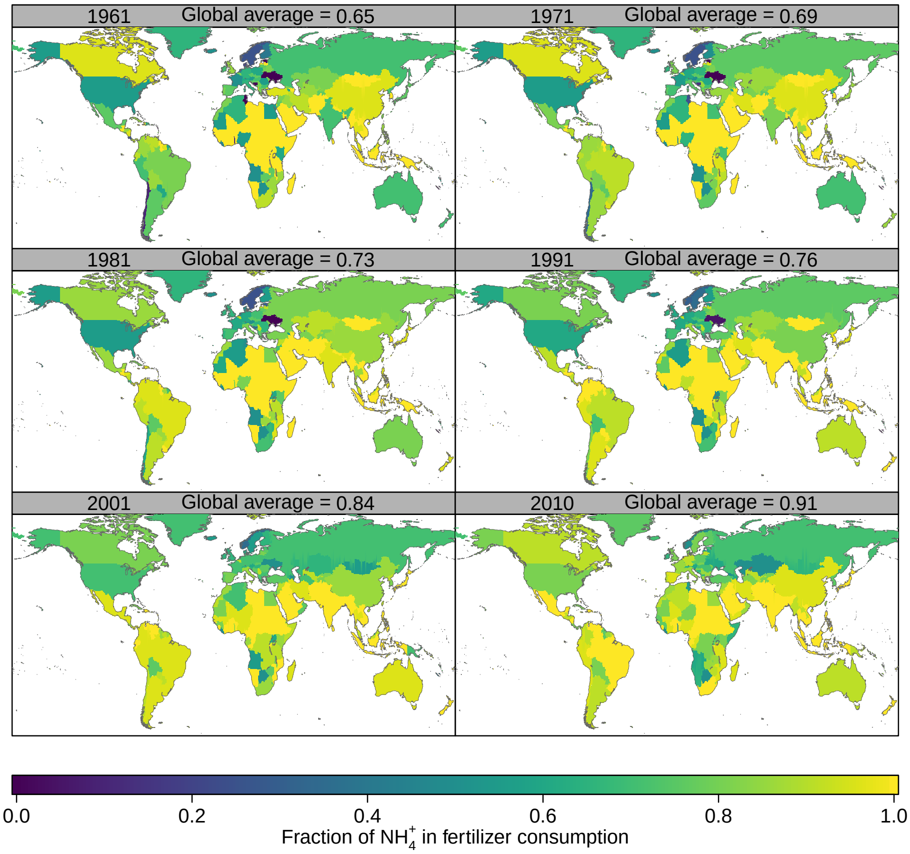

Figure 6. Fraction of NH_4^+ in N fertilizer input map during 1961–2010.

vantage of relevant information (population, GDP, and cropland area), which retains smoothness in the time-series information over time. In this way, the use of multiple imputation meant that we were able to generate consecutive time-series fertilizer inputs for all countries existing between 1961 and 2010.

However, in some countries (e.g., Somalia and Uzbekistan in Fig. 3), the imputed data did not smoothly follow the time series of national N fertilizer consumption. This was partially because of the abrupt changes in the observed values of those time series. Changes unrelated to the covariants (i.e., population, crop area) might reduce the accuracy of imputation of missing data. In fact, we occasionally observed some artifacts even in the reported values (e.g., the sequence of equal values) for the developing countries. In the process of accounting and compiling various datasets, there are inherent uncertainties in the national statistics (Leip, 2010; Winiwarter and Muik, 2010). Such uncertainties could also affect the quality of imputed data; hence, it should be noted that our dataset includes this inevitable uncertainty.

3.2 Comparison with existing N fertilizer map

We compared a new map for the year 2000 with the existing global N fertilizer maps provided by Potter et al. (2010) (hereafter "Potter's map") and Lu and Tian (2016) in Fig. 4. On the basis of the global scale N fertilizer input, the range of fertilizer input rates in our map (99.9th quantile; 172 kg-N ha^{-1} yr^{-1}) generally agreed with the range in Potter's fertilizer map (99.9th quantile; 138 kg-N ha^{-1} yr^{-1}) and the values were well correlated with each other ($R = 0.83$) with no large biases (ME = 0.21 kg-N ha^{-1} and RMSE = 3.92 kg-N ha^{-1}). In addition, we found general agreement ($R = 0.84$, ME = −0.08 kg-N ha^{-1} and RMSE = 3.93 kg-N ha^{-1}) with the N fertilizer map developed by Lu and Tian (2016). For the global total N input, our study's value in 2000 was 85 Tg-N yr^{-1}, which was larger than the global total inputs in other studies (70 Tg-N yr^{-1} in Potter et al., 2010; 80 Tg-N yr^{-1} in Lu and Tian, 2016, and 77.8 Tg-N yr^{-1} in Mueller et al., 2012). Without the imputed values, the global total N input was 81 Tg-N in 2000 in FAOSTAT. The major difference between our map and other maps is in the handling of cropping species. A bottom-up approach was taken to produce Potter's map; i.e., crop-specific fertilizer rates were first addressed and the map was produced as a summation of all crops us-

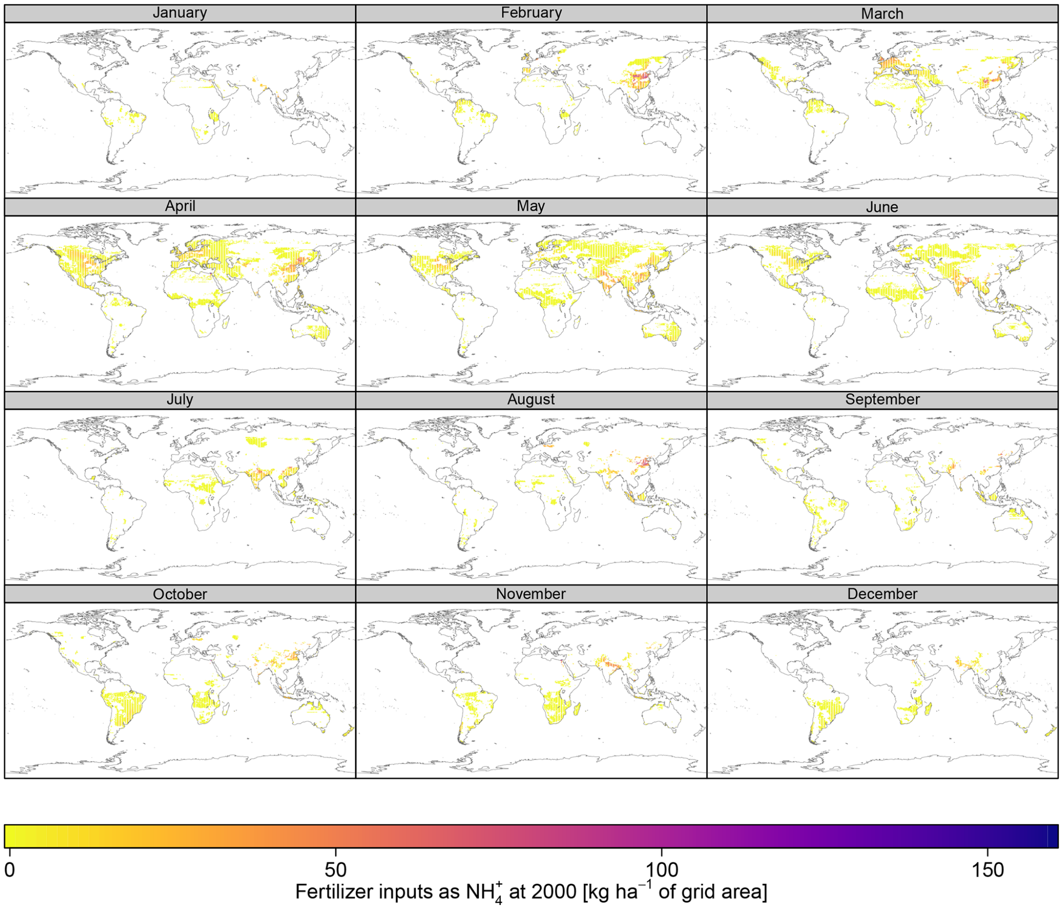

Figure 7. Monthly N fertilizer input as NH_4^+ in year 2000. Values represent average N applied over all crops across each $0.5° \times 0.5°$ grid cell.

ing each crop cultivation area map. In our study, we determined the values based only on national consumption data in FAOSTAT. In addition, the statistics in our map are based on FAOSTAT, whereas Potter et al. (2010) mainly used the International Fertilizer Industry Association (IFA) database (http://www.fertilizer.org/statistics) as a primary information source. An additional difference is that we applied statistical data imputation to the missing data. These discrepancies yielded the 11 Tg-N difference in total N fertilizer consumption in the global outcome.

With attention to spatial differences (Fig. 4), there were clear positive and negative differences in specific countries that have large cropland areas (i.e., United States, China, and India). In our map, N fertilizer input in India shows generally higher values than those in Potter's map. In China and USA, positive and negative differences were observed regionally. Potter's fertilizer map was based on the bottom-up approach with weighted crop-specific N fertilizer inputs; therefore, N fertilizer inputs are reflected in the spatial cropping distributions of each cropping species of the M3-Crops database (Monfreda et al., 2008). Also, there are differences in the cropland area maps; we used Hurtt et al. (2011) in this study, whereas Potter et al. (2010) used Ramankutty and Foley (1999). This also resulted in spatial contrasts between the two maps. In addition, there are differences in the treatment of double cropping regions. Potter's map did not consider the double cropping regions in the estimation of fertilizer inputs. These differences should be considered as uncertainty sources when the map is used.

3.3 Spatial and temporal patterns of $NH_4^+ : NO_3^-$ ratio in the fertilizer map

The NH_4^+ / NO_3^- ratio in national fertilizer varied considerably both geographically and temporally (Figs. 5–9). From the NH_4^+ / NO_3^- ratios among the regions (Fig. 6) and individual countries (Fig. 7), certain distinct features are noticeable. For example, Chile shows an almost 100 % NO_3^- fraction in the 1960s (Fig. 7). This is because Chilean nitrate made from desert minerals was the main source of N fertilizer product in this period. This is a particularly striking example; however, we can see the relatively high NO_3^- fraction all over Latin America during this period (Fig. 6). Such types of N fertilizer were gradually replaced by urea, thus ex-

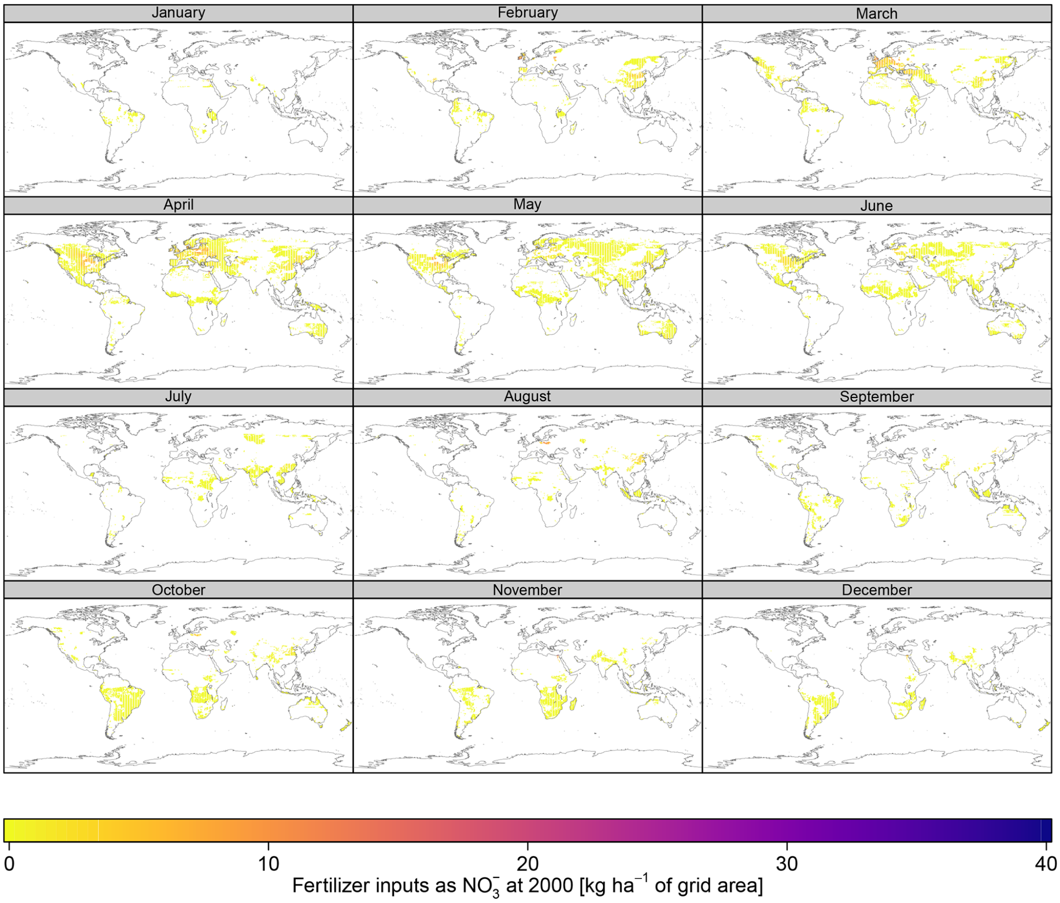

Figure 8. Monthly N fertilizer input as NO_3^- in year 2000. Values represent average N applied over all crops across each 0.5° × 0.5° grid cell.

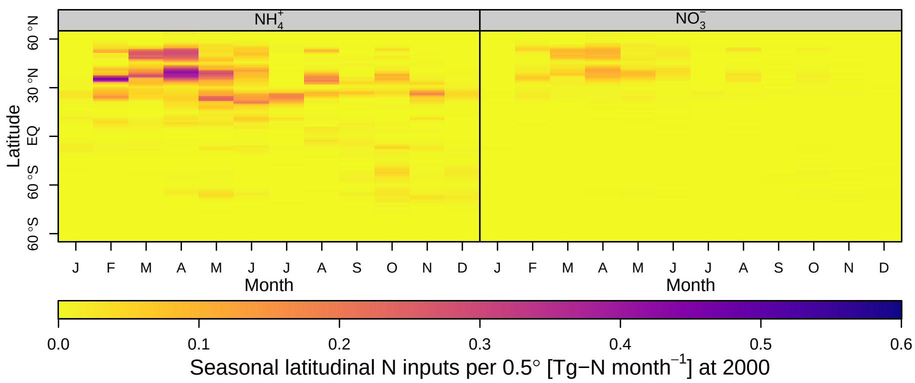

Figure 9. Fraction of NH_4^+ in N fertilizer input map during 1961–2010.

plaining the increase in the NH_4^+ fraction in this period. On the other hand, North America (United States and Canada) shows a lower NH_4^+ fraction during the entire period. In Asia, China and India show high NH_4^+ fractions during 1961–2010. China mainly consumed ammonium-forming fertilizers such as urea and ammonium bicarbonate ("Other N" in FAOSTAT) (Zhang et al., 2011). Likewise, India mainly consumed urea, ammonium phosphate, and ammonium sulfate nitrate; these are NH_4^+-forming N fertilizers.

Because of the differences in the NH_4^+ / NO_3^- ratio among the countries, there are spatio-seasonal differences in the NH_4^+ and NO_3^- inputs throughout the course of a year (Figs. 7–9). During February–March, both inputs exhibit a peak in the Northern Hemisphere, especially between 30 and

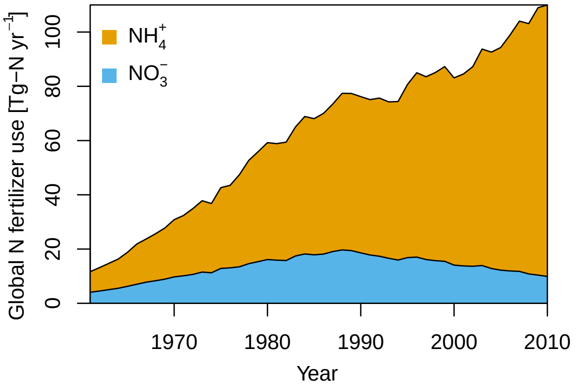

Figure 10. Estimated global N fertilizer use as NH_4^+ and NO_3^- inputs based on the sum of the imputed dataset. Orange and blue fractions indicate NH_4^+ and NO_3^-, respectively.

60° N (Fig. 9). For the tropics (from the Equator to 30° N), both inputs are observed throughout the year. In contrast, in the Southern Hemisphere, NH_4^+ inputs are dominantly observed during September and October in Fig. 9. This is because NO_3^- inputs in the Southern Hemisphere countries are a small fraction of the total N fertilizer inputs (Fig. 8). For the double cropping regions (Fig. 1), there are second peaks in both the NH_4^+ and NO_3^- inputs around 30° N (Fig. 9), particularly in south China and India (Figs. 7 and 8).

The global total N fertilizer input based on the sum of the dataset filled by imputation shows rapid increases during 1961–2010, reaching 110 Tg-N in 2010 (Fig. 10). The historical changes in NH_4^+ and NO_3^- inputs show different trends from the global total input. The estimated global total NO_3^- input peaked in 1989 (19.7 Tg-N year^{-1}) and decreased to 9.9 Tg-N yr^{-1} in 2010. From 1961 to 2010, the fraction of NO_3^- to total N fertilizer input consistently decreased from 35 to 13 % globally. On the other hand, the total amount and fraction of NH_4^+ increased consistently during the same period (Fig. 10). This is because of the expansion of the countries with high NH_4^+ consumption during this period, rather than the changes in $NH_4^+ : NO_3^-$ ratio in each country (Fig. 5).

3.4 Comparison of N deposition with NH_4^+ and NO_3^- inputs

N fertilizer and N deposition are the most important sources of disturbance of terrestrial N cycling (Gruber and Galloway, 2008). Although both inputs (finally) were comprised of NH_4^+ and NO_3^-, there has as yet been no quantitative comparison of these two inputs at global. Here, we compared differences in the historical geographic distribution between our map and terrestrial N deposition (Shindell et al., 2013) for terrestrial NH_4^+ and NO_3^- inputs. During the study period, the global annual N deposition increased from 41.9 to 67.1 Tg-N (Fig. 11) and the global annual N fertilizer input increased from 11.7 to 110.0 Tg-N (Fig. 10). The order of total inputs between the two Nr sources was comparable, but the rate of increase in N fertilizer input (2.43 Tg-N yr^{-1}) was higher than that of N deposition (0.63 Tg-N yr^{-1}). During the period, the global annual N deposition as NO_3^- inputs ranged from 19.4 to 31.1 Tg-N and annual global NO_3^- inputs by fertilizer ranged from 4.1 to 19.7 Tg-N (Fig. 10). Therefore, global total NO_3^- inputs from N fertilizer were consistently lower than those from N deposition.

In most latitudinal zones, total N fertilizer inputs increased due to the increase in N fertilizer consumption accompanied by crop area expansion during 1960–2010 (Fig. 11). A similar trend is seen in NH_4^+ fertilizer input. On the other hand, the amount of latitudinal NO_3^- input in N fertilizer in 2001 became smaller compared to that in 1991. In particular, in 45 to 55° N, NO_3^- input decreased from 6.4 to 4.4 Tg-N and further decreased to 3.2 Tg-N by 2010 (data not shown). However, this is still of a comparable order to NO_3^- deposition from latitudinal inputs in the temperate to cool temperate regions of the Northern Hemisphere.

4 Data availability

All products (NH_4^+ input, NO_3^- input, fraction of NH_4^+ to total inputs, and dates for fertilizer input) are provided in NetCDF format at https://doi.pangaea.de/10.1594/PANGAEA.861203.

5 Conclusion and remarks

Overall, using the statistical imputation, we were able to generate a filled dataset for national fertilizer consumption for all the countries in the FAOSTAT database between 1961 and 2010. This procedure also enabled us to estimate the fraction of NH_4^+ (NO_3^-) in the total N fertilizer inputs based on chemical fertilizer information.

The products proposed in this paper could be widely utilized for global N cycling studies such as N gas emission (e.g., Hudman et al., 2012) and N leaching (e.g., He et al., 2011) on a global scale. We have a few options for the historical global N fertilizer map at present (e.g., Lu and Tian, 2016), even though global N cycling is paid attention from various study fields. Hence, this map could be an alternative option for estimating historical N fertilizer inputs in global model studies, although the N dose in our map is based on a simple balance equation using national consumption data and cropland area.

The ratio of NH_4^+ to NO_3^- in N fertilizer has not been considered in earlier biogeochemical models for global N cycling. The ratio of NO_3^- to total N fertilizer inputs decreased with time from 1961 to 2010; however, the amount of NO_3^- as a fertilizer input is still comparable with terrestrial NO_3^- deposition. In fertilized soils, NH_4^+ and NO_3^- affect biogeochemical processes (e.g., nitrification and denitrifica-

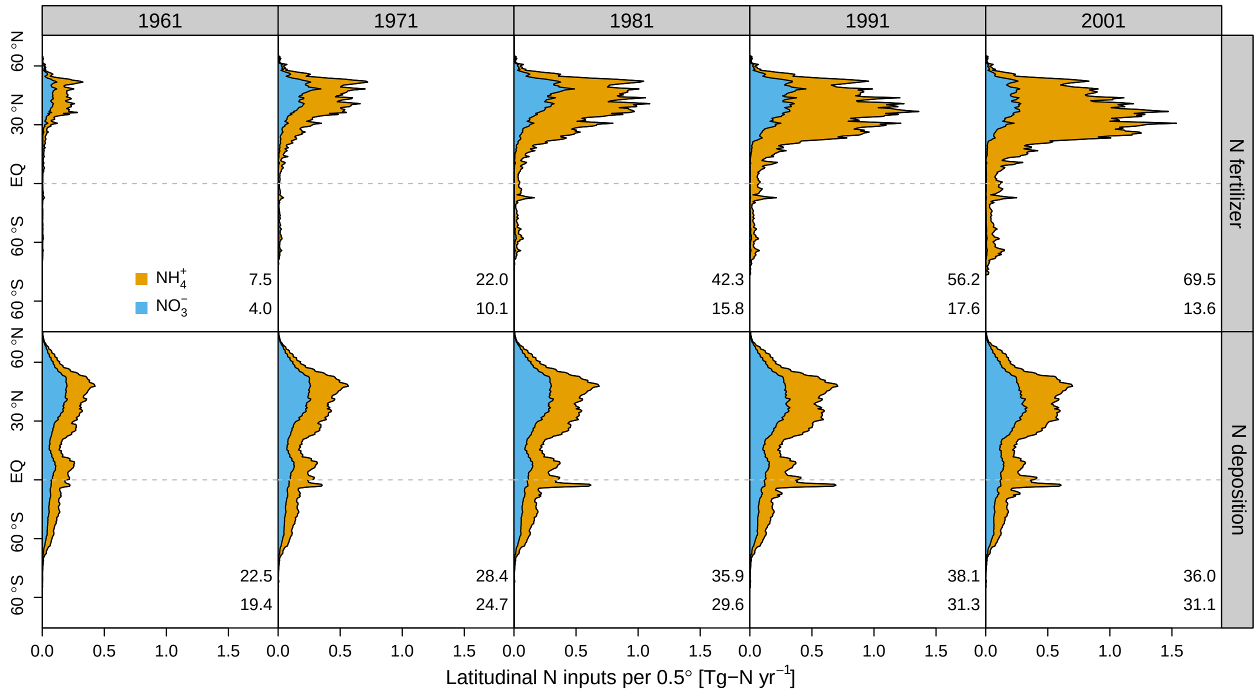

Figure 11. Latitudinal NH_4^+ and NO_3^- inputs to terrestrial land area from N fertilizer (upper) and N deposition (lower). Values represent the sum of N inputs at each 0.5° resolution. N deposition is from ACCMIP study (Shindell et al., 2013). Orange and blue fractions in each plot indicate NH_4^+ and NO_3^-, respectively. The values inside each plot indicate global total input of NH_4^+ (upper) and NO_3^- (lower) to terrestrial land area.

tion). Thus, in relation to NO_3^-, our map offers new insights into terrestrial N inputs and impacts from synthetic fertilizer.

The national census has inherent uncertainty, even in the existing activity data (Winiwarter and Muik, 2010). Therefore, to some extent, this N fertilizer map also has unavoidable uncertainties. For example, using this map as a prior distribution, inverse modeling studies with atmospheric N concentrations (e.g., Thompson et al., 2014a, b) might enable us to improve and update the accuracy of the N fertilizer map.

The map of the ratio of NH_4^+ to NO_3^- in N fertilizer is also provided, and this information could be used in the existing N fertilizer maps.

Competing interests. The authors declare that they have no conflict of interest.

Acknowledgements. With great respect, K. Nishina expresses appreciation for all data providers for their effort in developing and sharing valuable datasets. We also wish especially to thank S. Siebert at Bonn University for kindly sharing the crop use intensity map. Our work is based entirely on these resources; we hope to have added value to these existing datasets, especially to the biogeochemical modeling communities. Furthermore, we would like to express our appreciation to editor D. Carlson, anonymous reviewers, and C. Lu (Iowa State University) for valuable comments on our manuscript and dataset. This work is partially supported by the Environment Research and Technology Development Fund (S-10) of the Ministry of the Environment, Japan.

Edited by: D. Carlson
Reviewed by: two anonymous referees

References

Bouwman, A.: Direct emission of nitrous oxide from agricultural soils, Nutr. Cycl. Agroecosys., 46, 53–70, 1996.

Bouwman, A., Boumans, L., and Batjes, N.: Estimation of global NH_3 volatilization loss from synthetic fertilizers and animal manure applied to arable lands and grasslands, Global Biogeochem. Cy., 16, doi:10.1029/2000GB001389, 2002.

Bouwman, L., Goldewijk, K. K., Van Der Hoek, K. W., Beusen, A. H., Van Vuuren, D. P., Willems, J., Rufino, M. C., and Stehfest, E.: Exploring global changes in nitrogen and phosphorus cycles in agriculture induced by livestock production over the 1900–2050 period, P. Natl. Acad. Sci. USA, 110, 20882–20887, 2013.

Conant, R. T., Berdanier, A. B., and Grace, P. R.: Patterns and trends in nitrogen use and nitrogen recovery efficiency in world agriculture, Global Biogeochem. Cy., 27, 558–566, 2013.

Davidson, E. A.: The contribution of manure and fertilizer nitrogen to atmospheric nitrous oxide since 1860, Nat. Geosci., 2, 659–662, 2009.

Davidson, E. A.: Representative concentration pathways and mitigation scenarios for nitrous oxide, Environ. Res. Lett., 7, 024005, doi:10.1088/1748-9326/7/2/024005, 2012.

De Vries, W., Kros, J., Kroeze, C., and Seitzinger, S. P.: Assessing planetary and regional nitrogen boundaries related to food security and adverse environmental impacts, Current Opinion in Environmental Sustainability, 5, 392–402, 2013.

Erisman, J. W., Sutton, M. A., Galloway, J., Klimont, Z., and Winiwarter, W.: How a century of ammonia synthesis changed the world, Nat. Geosci., 1, 636–639, 2008.

Evans, M. D., Kelley, J., Sikora, J., and Treiman, D. J.: Family scholarly culture and educational success: Books and schooling in 27 nations, Research in Social Stratification and Mobility, 28, 171–197, 2010.

Food and Agriculture Organization of the United Nations: FAOSTAT (Database), latest update: 7 March 2014, available at: http://data.fao.org/ref/262b79ca-279c-4517-93de-ee3b7c7cb553.html?version=1.0, last access: 10 September 2014.

Galloway, J. N., Aber, J. D., Erisman, J. W., Seitzinger, S. P., Howarth, R. W., Cowling, E. B., and Cosby, B. J.: The nitrogen cascade, Bioscience, 53, 341–356, 2003.

Galloway, J. N., Dentener, F. J., Capone, D. G., Boyer, E. W., Howarth, R. W., Seitzinger, S. P., Asner, G. P., Cleveland, C., Green, P., Holland, E., Karl, D. M., Michaels, A. F., Porter, J. H., Townsend, A. R., and Vöosmarty, C. J.: Nitrogen cycles: past, present, and future, Biogeochemistry, 70, 153–226, 2004.

Galloway, J. N., Townsend, A. R., Erisman, J. W., Bekunda, M., Cai, Z., Freney, J. R., Martinelli, L. A., Seitzinger, S. P., and Sutton, M. A.: Transformation of the nitrogen cycle: recent trends, questions, and potential solutions, Science, 320, 889–892, 2008.

Gruber, N. and Galloway, J. N.: An Earth-system perspective of the global nitrogen cycle, Nature, 451, 293–296, 2008.

Harrison, R. and Webb, J.: A review of the effect of N fertilizer type on gaseous emissions, Adv. Agro., 73, 65–108, 2001.

He, B., Kanae, S., Oki, T., Hirabayashi, Y., Yamashiki, Y., and Takara, K.: Assessment of global nitrogen pollution in rivers using an integrated biogeochemical modeling framework, Water Res., 45, 2573–2586, 2011.

Honaker, J. and King, G.: What to do about missing values in time-series cross-section data, Am. J. Polit. Sci., 54, 561–581, 2010.

Honaker, J., King, G., and Blackwell, M.: Amelia II: A program for missing data, J. Stat. Softw., 45, 1–47, 2011.

Hudman, R. C., Moore, N. E., Mebust, A. K., Martin, R. V., Russell, A. R., Valin, L. C., and Cohen, R. C.: Steps towards a mechanistic model of global soil nitric oxide emissions: implementation and space based-constraints, Atmos. Chem. Phys., 12, 7779–7795, doi:10.5194/acp-12-7779-2012, 2012.

Hurtt, G., Chini, L. P., Frolking, S., Betts, R., Feddema, J., Fischer, G., Fisk, J., Hibbard, K., Houghton, R., Janetos, A., Jones, C. D., Kindermann, G., Kinoshita, T., Klein Goldewijk, K., Riahi, K., Shevliakova, E., Smith, S., Stehfest, E., Thomson, A., Thornton, P., van Vuuren, D. P., Wang, Y. P.: Harmonization of land-use scenarios for the period 1500–2100: 600 years of global gridded annual land-use transitions, wood harvest, and resulting secondary lands, Climatic Change, 109, 117–161, 2011.

King, G., Honaker, J., Joseph, A., and Scheve, K.: Analyzing incomplete political science data: An alternative algorithm for multiple imputation, in: American Political Science Association, vol. 95, 49–69, Cambridge Univ Press, 2001.

Leip, A.: Quantitative quality assessment of the greenhouse gas inventory for agriculture in Europe, Climatic Change, 103, 245–261, doi:10.1007/s10584-010-9915-5, 2010.

Liu, J., You, L., Amini, M., Obersteiner, M., Herrero, M., Zehnder, A. J., and Yang, H.: A high-resolution assessment on global nitrogen flows in cropland, P. Natl. Acad. Sci. USA, 107, 8035–8040, 2010.

Lu, C. and Tian, H.: Global nitrogen and phosphorus fertilizer use for agriculture production in the past half century: Shifted hot spots and nutrient imbalance, Earth Syst. Sci. Data Discuss., doi:10.5194/essd-2016-35, in review, 2016.

Matthews, E.: Nitrogenous fertilizers: Global distribution of consumption and associated emissions of nitrous oxide and ammonia, Global Biogeochem. Cy., 8, 411–439, doi:10.1029/94GB01906, 1994.

Monfreda, C., Ramankutty, N., and Foley, J. A.: Farming the planet: 2. Geographic distribution of crop areas, yields, physiological types, and net primary production in the year 2000, Global Biogeochem. Cy., 22, GB1022, doi:10.1029/2007GB002947, 2008.

Mosier, A., Kroeze, C., Nevison, C., Oenema, O., Seitzinger, S., and Van Cleemput, O.: Closing the global N_2O budget: nitrous oxide emissions through the agricultural nitrogen cycle, Nutr. Cycl. Agroecosys., 52, 225–248, 1998.

Mueller, N. D., Gerber, J. S., Johnston, M., Ray, D. K., Ramankutty, N., and Foley, J. A.: Closing yield gaps through nutrient and water management, Nature, 490, 254–257, 2012.

Potter, P., Ramankutty, N., Bennett, E. M., and Donner, S. D.: Characterizing the spatial patterns of global fertilizer application and manure production, Earth Interact., 14, 1–22, 2010.

Pyšek, P., Manceur, A. M., Alba, C., McGregor, K. F., Pergl, J., Štajerová, K., Chytr, M., Danihelka, J., Kartesz, J., Klimešová, J., Lučanová, M., Moravcová, L., Nishino, M., Sádlo, J., Suda, J., Tich, L., and Kühn, I.: Naturalization of central European plants in North America: species traits, habitats, propagule pressure, residence time, Ecology, 96, 762–774, 2015.

Ramankutty, N. and Foley, J. A.: Estimating historical changes in global land cover: Croplands from 1700 to 1992, Global Biogeochem. Cy., 13, 997–1027, 1999.

Rockström, J., Steffen, W., Noone, K., Persson, Å., Chapin, F. S., Lambin, E. F., Lenton, T. M., Scheffer, M., Folke, C., Schellnhuber, H. J., Nykvist, B., de Wit, C. A., Hughes, T., Van Der Leeuw, S., Rodhe, H., Srlin, S., Snyder, P. K., Constanza, R., Svedin, U., Falkenmark, M, Karlberg, L., Corell, R. W., Fabry, V. J., Hansen, J., Walker, B., Livermann, D., Richardson, K., Crutzen, P. J., and Foley, J: A safe operating space for humanity, Nature, 461, 472–475, 2009.

Ross, M.: Is democracy good for the poor?, Am. J. Polit. Sci., 50, 860–874, 2006.

Sacks, W. J., Deryng, D., Foley, J. A., and Ramankutty, N.: Crop planting dates: an analysis of global patterns, Global Ecol. Biogeogr., 19, 607–620, 2010.

Shcherbak, I., Millar, N., and Robertson, G. P.: Global metaanalysis of the nonlinear response of soil nitrous oxide (N_2O) emissions to fertilizer nitrogen, P. Natl. Acad. Sci. USA, 111, 9199–9204, 2014.

Shindell, D. T., Lamarque, J.-F., Schulz, M., Flanner, M., Jiao, C., Chin, M., Young, P. J., Lee, Y. H., Rotstayn, L., Mahowald, N., Milly, G., Faluvegi, G., Balkanski, Y., Collins, W. J., Conley, A. J., Dalsoren, S., Easter, R., Ghan, S., Horowitz, L., Liu, X., Myhre, G., Nagashima, T., Naik, V., Rumbold, S. T., Skeie, R., Sudo, K., Szopa, S., Takemura, T., Voulgarakis, A., Yoon, J.-H., and Lo, F.: Radiative forcing in the ACCMIP historical and future climate simulations, Atmos. Chem. Phys., 13, 2939–2974, doi:10.5194/acp-13-2939-2013, 2013.

Siebert, S., Portmann, F. T., and Döll, P.: Global patterns of cropland use intensity, Remote Sensing, 2, 1625–1643, doi:10.3390/rs2071625, 2010.

Steffen, W. and Smith, M. S.: Planetary boundaries, equity and global sustainability: why wealthy countries could benefit from more equity, Current Opinion in Environmental Sustainability, 5, 403–408, 2013.

Steffen, W., Richardson, K., Rockström, J., Cornell, S. E., Fetzer, I., Bennett, E. M., Biggs, R., Carpenter, S. R., de Vries, W., de Wit, C. A., Folke, C., Gerten, D., Heinke, J., Mace, G. M., Persson, L. M., Ramanathan, V., Reyers, B., and Sörlin, S.: Planetary boundaries: Guiding human development on a changing planet, Science, 347, 1259855, doi:10.1126/science.1259855, 2015.

Sutton, M. A. and Bleeker, A.: Environmental science: the shape of nitrogen to come, Nature, 494, 435–437, 2013.

Thompson, R. L., Ishijima, K., Saikawa, E., Corazza, M., Karstens, U., Patra, P. K., Bergamaschi, P., Chevallier, F., Dlugokencky, E., Prinn, R. G., Weiss, R. F., O'Doherty, S., Fraser, P. J., Steele, L. P., Krummel, P. B., Vermeulen, A., Tohjima, Y., Jordan, A., Haszpra, L., Steinbacher, M., Van der Laan, S., Aalto, T., Meinhardt, F., Popa, M. E., Moncrieff, J., and Bousquet, P.: TransCom N_2O model inter-comparison – Part 2: Atmospheric inversion estimates of N_2O emissions, Atmos. Chem. Phys., 14, 6177–6194, doi:10.5194/acp-14-6177-2014, 2014a.

Thompson, R. L., Patra, P. K., Ishijima, K., Saikawa, E., Corazza, M., Karstens, U., Wilson, C., Bergamaschi, P., Dlugokencky, E., Sweeney, C., Prinn, R. G., Weiss, R. F., O'Doherty, S., Fraser, P. J., Steele, L. P., Krummel, P. B., Saunois, M., Chipperfield, M., and Bousquet, P.: TransCom N_2O model inter-comparison – Part 1: Assessing the influence of transport and surface fluxes on tropospheric N_2O variability, Atmos. Chem. Phys., 14, 4349–4368, doi:10.5194/acp-14-4349-2014, 2014b.

Tian, H., Lu, C., Ciais, P., Michalak, A. M., Canadell, J. G., Saikawa, E., Huntzinger, D. N., Gurney, K. R., Sitch, S., Zhang, B., Yang, J., Bousquet, P., Bruhwiler, L., Chen, G., Dlugokencky, E., Friedlingstein, P., Melillo, J., Pan, S., Poulter, B., Prinn, R., Saunois, M., Schwalm, C. R., and Wofsy, S. C.: The terrestrial biosphere as a net source of greenhouse gases to the atmosphere, Nature, 531, 225–228, 2016.

Winiwarter, W. and Muik, B.: Statistical dependence in input data of national greenhouse gas inventories: effects on the overall inventory uncertainty, Climatic Change, 103, 19–36, 2010.

Zhang, Y., Luan, S., Chen, L., and Shao, M.: Estimating the volatilization of ammonia from synthetic nitrogenous fertilizers used in China, J. Environ. Manage., 92, 480–493, 2011.